


## RESEARCH ARTICLE

# Cleavage efficiency of the intramembrane protease $\gamma$ -secretase is reduced by the palmitoylation of a substrate's transmembrane domain

Marlene Aßfalg<sup>1,2</sup> | Gökhan Güner<sup>1,2</sup> | Stephan A. Müller<sup>1,2</sup> |  
Stephan Breimann<sup>1,2,3,4</sup> | Dieter Langosch<sup>5</sup> | Claudia Muhle-Goll<sup>6</sup> |  
Dmitrij Frishman<sup>3</sup> | Harald Steiner<sup>1,4</sup> | Stefan F. Lichtenthaler<sup>1,2,7</sup> 

<sup>1</sup>German Center for Neurodegenerative Diseases (DZNE), Munich, Germany

<sup>2</sup>Neuroproteomics, School of Medicine and Health, Klinikum rechts der Isar, Technical University of Munich, Munich, Germany

<sup>3</sup>Department of Bioinformatics, School of Life Sciences, Technical University of Munich, Freising, Germany

<sup>4</sup>Biomedical Center (BMC), Division of Metabolic Biochemistry, Faculty of Medicine, LMU Munich, Munich, Germany

<sup>5</sup>Technical University of Munich, Freising, Germany

<sup>6</sup>Institute for Biological Interfaces 4, Karlsruhe Institute of Technology, Eggenstein-Leopoldshafen, Germany

<sup>7</sup>Munich Cluster for Systems Neurology (SyNergy), Munich, Germany

## Correspondence

Stefan F. Lichtenthaler, German  
Center for Neurodegenerative Diseases  
(DZNE), Feodor-Lynen-Str. 17, Munich  
81377, Germany.  
Email: [stefan.lichtenthaler@dzne.de](mailto:stefan.lichtenthaler@dzne.de)

## Funding information

Deutsche Forschungsgemeinschaft  
(DFG), Grant/Award Number:  
263531414/FOR2290, MU1606/6-2  
and EXC 2145 SyNergy- ID 390857198;  
Helmholtz HGF, Grant/Award Number:  
43.35.02

## Abstract

The intramembrane protease  $\gamma$ -secretase has broad physiological functions, but also contributes to Notch-dependent tumors and Alzheimer's disease. While  $\gamma$ -secretase cleaves numerous membrane proteins, only few nonsubstrates are known. Thus, a fundamental open question is how  $\gamma$ -secretase distinguishes substrates from nonsubstrates and whether sequence-based features or post-translational modifications of membrane proteins contribute to substrate recognition. Using mass spectrometry-based proteomics, we identified several type I membrane proteins with short ectodomains that were inefficiently or not cleaved by  $\gamma$ -secretase, including 'pituitary tumor-transforming gene 1-interacting protein' (PTTG1IP). To analyze the mechanism preventing cleavage of these putative nonsubstrates, we used the validated substrate FN14 as a backbone and replaced its transmembrane domain (TMD), where  $\gamma$ -cleavage occurs, with the one of non-substrates. Surprisingly, some nonsubstrate TMDs were efficiently cleaved in the FN14 backbone, demonstrating that a cleavable TMD is necessary, but not sufficient for cleavage by  $\gamma$ -secretase. Cleavage efficiencies varied by up to 200-fold.

**Abbreviations:** AD, Alzheimer's disease; APP, amyloid precursor protein; C99, 99 amino acid long C-terminal fragment of APP; DAPT,  $\gamma$ -secretase inhibitor N-[N-(3,5-difluorophenacetyl)-L-alanyl]-S-phenylglycine *t*-butyl ester; FXYD3, FXYD domain-containing ion transport regulator 3; PS, presenilin; PTTG1IP, pituitary tumor-transforming gene 1-interacting protein; TMD, transmembrane domain.

Marlene Aßfalg and Gökhan Güner contributed equally to this work.

This is an open access article under the terms of the [Creative Commons Attribution-NonCommercial](https://creativecommons.org/licenses/by/4.0/) License, which permits use, distribution and reproduction in any medium, provided the original work is properly cited and is not used for commercial purposes.

© 2024 The Authors. *The FASEB Journal* published by Wiley Periodicals LLC on behalf of Federation of American Societies for Experimental Biology.

Other TMDs, including that of PTTG1IP, were still barely cleaved within the FN14 backbone. Pharmacological and mutational experiments revealed that the PTTG1IP TMD is palmitoylated, which prevented cleavage by  $\gamma$ -secretase. We conclude that the TMD sequence of a membrane protein and its palmitoylation can be key factors determining substrate recognition and cleavage efficiency by  $\gamma$ -secretase.

#### KEYWORDS

FXYD3, FXYD6, intramembrane proteolysis, LYRIC, PMEPA1, protease substrate specificity, TNR12, Tweak receptor

## 1 | INTRODUCTION

Intramembrane proteases have fundamental functions in all kingdoms of life, ranging from membrane protein homeostasis to control of cellular metabolism and the communication between cells in multicellular organisms.<sup>1-4</sup> These proteases cleave their membrane protein substrates within or very close to their transmembrane domains (TMDs) and exist as aspartyl-, serine- or metalloproteases, depending on their catalytic mechanism. Among the aspartyl intramembrane proteases,  $\gamma$ -secretase has been studied most intensively, because of its role in Notch signaling during development, in Notch-dependent tumors and in Alzheimer's disease (AD),<sup>5</sup> where  $\gamma$ -secretase cleaves the amyloid precursor protein (APP) and generates the pathogenic amyloid  $\beta$  (A $\beta$ ) peptide.  $\gamma$ -Secretase is a heterotetrameric protein complex consisting of one proteolytically active subunit, presenilin (PS), and three non-proteolytic subunits nicastrin, APH-1 (anterior pharynx defective-1) and presenilin enhancer 2 (PEN-2).<sup>6</sup>

$\gamma$ -Secretase inhibitors are tested for treatment of Notch-dependent tumors, including desmoid tumors and T-cell acute lymphoblastic leukemia.<sup>7,8</sup> Previously, they were also tested for a treatment of AD, but were discontinued because of the occurrence of mechanism-based side effects, resulting from inhibition of other  $\gamma$ -secretase substrates, such as Notch and potentially others.<sup>9,10</sup> Beyond Notch and APP,  $\gamma$ -secretase cleaves approximately 150 additional membrane proteins.<sup>11</sup> Despite this large number, a fundamental open question is to understand which features of a membrane protein distinguish substrates from nonsubstrates, i.e. membrane proteins that are not cleaved by  $\gamma$ -secretase or cleaved with low efficiency. Elucidating such features is essential to better understand the mechanism of how substrates among the more than 1000 type I membrane proteins in the human proteome are recognized, bound and cleaved and to potentially enable substrate-specific inhibition of  $\gamma$ -secretase for development of safer drugs for AD and other diseases.

Some requirements for substrate cleavage by  $\gamma$ -secretase are known from the comparison of the known substrates and from mechanistic studies. All known  $\gamma$ -secretase substrates are single-span transmembrane proteins with a type I orientation, i.e. an extracellular N-terminus and a cytosolic C-terminus.<sup>11</sup>  $\gamma$ -Secretase does not cleave with a pronounced sequence specificity, but may rather require structural flexibility within a substrate's TMD.<sup>12-14</sup> Additionally, membrane proteins require a short extracellular domain (ectodomain) to be recognized and cleaved by  $\gamma$ -secretase.<sup>15-17</sup> This prevents most known  $\gamma$ -secretase substrates from being constitutively cleaved, because they have long ectodomains. Before cleavage by  $\gamma$ -secretase they need to undergo ectodomain shedding, i.e. truncation of the ectodomain by other proteases.<sup>3</sup> Otherwise, their cleavage by  $\gamma$ -secretase will not take place or only with very low efficiency.<sup>18</sup> This length requirement is controlled by the  $\gamma$ -secretase subunit nicastrin, which has an ectodomain that forms a lid-like structure on top of the active site of  $\gamma$ -secretase and thus, prevents cleavage of proteins with long ectodomains.<sup>16,19,20</sup> As a consequence, most mechanistic studies with  $\gamma$ -secretase rely on the use of model substrates with artificially truncated ectodomains. An exception are three recently discovered  $\gamma$ -secretase substrates, the B cell maturation antigen (BCMA), the TWEAK receptor FN14 (also known as TWEAK receptor, TNR12, CD266 or Fibroblast growth factor-inducible protein 14) and synaptotagmin-7,<sup>21-23</sup> which do not require ectodomain shedding, because they have short ectodomains of 54 (BCMA), 53 (FN14) or 16 (Syt-7) amino acids. The three proteins constitute the emerging subfamily of naturally short  $\gamma$ -secretase substrates, which offer the advantage for mechanistic studies that their direct cleavage by  $\gamma$ -secretase can be monitored without interference by an initial ectodomain shedding step and that expression of pre-truncated forms of the proteins is not required.

Yet, a more thorough comparison of the features that distinguish substrates from nonsubstrates does not only require a list of validated substrates but also a list of

proteins that are not cleaved or only with low efficiency. However, while many substrates were identified, only very few nonsubstrates are known for  $\gamma$ -secretase, such as integrin  $\beta$  (ITGB1) and natriuretic peptide receptor A (NPR-A).<sup>24</sup>

Here, we focused on membrane proteins with naturally short ectodomains. Using mass spectrometry-based proteomics we identified and then validated several of them as nonsubstrates for  $\gamma$ -secretase, including 'pituitary tumor-transforming gene 1-interacting protein' (PTTG1IP). Because  $\gamma$ -secretase cleavage occurs within a substrate's TMD, we generated TMD swap mutants between the validated substrate FN14, which served as a model substrate, and several nonsubstrates. Cleavage efficiency of the domain swap mutants strongly depended on the TMD sequence. Further swaps of N- and C-terminal TMD halves and mutations of individual amino acids as well as pharmacological experiments identified substrate palmitoylation in the C-terminal half of the TMD as a feature that blocks  $\gamma$ -secretase cleavage.

## 2 | MATERIALS AND METHODS

### 2.1 | Culture of the cell line

DMEM (Gibco) supplemented with 10% FCS and 1% penicillin/streptomycin was used as the culture medium for Human embryonic kidney 293 EBNA cells (HEK293). Cells were regularly tested to be mycoplasma-free.

### 2.2 | Transfection of constructs in cell culture, 2-bromopalmitate treatment and Western blots

HEK293 cells were seeded on 12-well plates (Corning) and transfected with a pcDNA3.1 plasmid carrying the different plasma membrane constructs (FN14, FXYD3, FXYD6, PMEPA1 and PTTG1IP full length, LYRIC and SYT12 with a shortened cytoplasmic tail: amino acid 1–104 and AA 1–95, respectively, and ITGB1 with a shortened N-terminus, amino acids AA 703–798 to keep the construct sizes similar) tagged with an N-terminal HA-tag (YPYDVPDYA) and a C-terminal double FLAG tag with a three amino acid linker (GLEDYKDDDDKDYKDDDDK) as described before.<sup>23</sup> Shortly, transfection was performed by Lipofectamine™ 2000, according to the manufacturer's instructions (Thermo Fisher, US). Cells were incubated overnight in 1 mL DMEM (Gibco) with 10% FCS, containing either 1  $\mu$ M of the  $\gamma$ -secretase inhibitor DAPT (Sigma) or DMSO as control. For palmitoylation inhibition, 50  $\mu$ M 2-bromo palmitate (Sigma) or DMSO as control were used

for overnight treatment. Conditioned media were collected and centrifuged for 1 h at 100000g and stored at  $-20^{\circ}\text{C}$ . Cells were lysed with 100  $\mu$ L STET (150 mM NaCl, 50 mM Tris [pH 7.5], 2 mM EDTA, 1% Triton X-100) buffer containing 1 $\times$  protease inhibitor (Sigma). The lysate and the correspondingly adjusted volume of conditioned media were loaded on Schagger gradient gels.<sup>25</sup> For side-by-side loading of lysate and conditioned media, the lysate was diluted 1:100. Detection of overexpressed proteins and their proteolytic products was done with anti-HA.11 (Covance, clone 16B12, Cat MMS-101P) antibody.

### 2.3 | Conditioned medium enrichment

Either conditioned medium was directly loaded, adjusted to match the lysate volume, or it was immunoprecipitated with an anti-HA-tag antibody. To facilitate the enrichment process, 700  $\mu$ L of conditioned medium was incubated overnight with 5  $\mu$ L of Anti-HA magnetic beads (Pierce) at 4 $^{\circ}\text{C}$  with continuous shaking. Subsequently, the immunoprecipitant was eluted in 40  $\mu$ L of 1 $\times$  Laemmli buffer in STET through a 10-minute incubation at 95 $^{\circ}\text{C}$ . For gel electrophoresis, 30  $\mu$ L of the eluate (10  $\mu$ L for FN14) was loaded onto Schagger gradient gels, and detection was carried out using the anti-HA.11 antibody.

### 2.4 | Relative cleavage efficiency determination

Densitometry quantification of Western blots was conducted using ImageLab software (Bio-Rad Laboratories, Version 6.1). The intensity of the A $\beta$ -like protein, which appeared at approximately 10 kDa in the conditioned media, was divided by the intensity of the full-length protein observed at approximately 20 kDa in the cell lysate. To establish a reliable baseline, this ratio was further normalized to the corresponding FN14 ratio, serving as a control for each blot. Finally, the logarithmic values of these normalized ratios were plotted, providing a visual representation of the relative cleavage efficiency in comparison to FN14.

### 2.5 | In vitro isolated membrane incubation assay to measure the $\gamma$ -secretase activity

The assay was performed as previously described.<sup>26</sup> Shortly, HEK293 cells were transfected with the epitope-tagged plasmids. The membranes were isolated and incubated in reaction buffer (150 mM sodium citrate pH 6.4

with 1× protease inhibitor), in the presence of either 1 μM DAPT or vehicle. The reaction was incubated at 37°C for 4 h. At the end of the reaction, samples were centrifuged at 100 000g for 1 h. Supernatants were boiled in Laemmli buffer, loaded on Schagger gels and blotted with the FLAG-M2 antibody (Sigma).

## 2.6 | Mass spectrometry-based proteomics

Four cell lines, HeLa, MCF7, Jurkat, and U937 were used in mass spectrometry experiments. Cell lines were cultured in T-175 flasks (Thermo). 24 h prior to collection, cells were treated with 1 μM DAPT or DMSO as control. Following number of replicates were analyzed: HeLa (4 DAPT, 5 DMSO), Jurkat (6 DAPT, 5 DMSO), MCF7 (5 DAPT, 5 DMSO), and U937 (4 DAPT, 5 DMSO). Adherent cell lines HeLa and MCF7 were suspended using 1 mM EDTA in PBS. Membrane fractions of the treated cells were collected as described.<sup>27</sup> In brief, collected cells were homogenized by 27-gauge needle in homogenization buffer (250 mM sucrose, 10 mM HEPES-KOH pH 7.4, 1 mM EDTA, 1x protease inhibitor). Homogenates were centrifuged at 750g for 10 min to remove nuclei, followed by 100 000g for 90 min to pellet the membrane. Membrane pellets were washed in 100 mM Na<sub>2</sub>CO<sub>3</sub>, and subsequently dissolved by sonication in STET buffer with 2% Triton X-100. The samples were prepared for MS analyses via filter-aided sample preparation (FASP) as described before<sup>28</sup> and digested with LysC and Trypsin (Promega, Germany).

The samples were analyzed by liquid chromatography tandem mass spectrometry (LC-MS/MS), with Easy nLC-1000 coupled to Q-Exactive mass spectrometer (Thermo Scientific Scientific) using a NanoFlex ion source equipped with an PRSO-V1 column oven (Sonation, Germany). Fused silica columns (30 cm × 75 μm, New Objective US) packed with 1.9 μm ReproSil-Pur 120 C18-AQ stationary phase (Dr. Maisch, Germany) were used for peptide separation. A binary gradient of water (A) and acetonitrile (B) supplemented with 0.1% formic acid were used (HeLa, MCF7, U937: 0 min., 2% B; 5 min., 5% B; 185 min., 25% B; 230 min, 35% B; 250 min, 60% B; 255 min.; Jurkat: 0 min., 2% B; 3:30 min., 5% B; 137:30 min., 25% B; 168:30 min., 35% B; 182:30 min., 60% B) at 50°C column temperature. A data-dependent acquisition method was used. An amount of 1 μg of digested peptide was injected per run. Full MS scans were acquired at a resolution of 70 000 (m/z range: 300–1400, AGC target: 3E+6). The 10 most intense peptide ions per full MS scan were chosen for peptide fragmentation (resolution: 17500, isolation width: 2.0 m/z,

AGC target: 1E+5, NCE: 25%). A dynamic exclusion of 120 s was used for peptide fragmentation.

## 2.7 | Mass spectrometric data analysis

MS results were analyzed by MaxQuant using label-free quantification (LFQ).<sup>29</sup> The data were searched against a one protein per gene canonical human database from UniProt (download: 2022-01-18; 20 600 entries). Trypsin was used as protease. Oxidation of methionines and acetylation of protein N-termini were defined as variable modifications, whereas carbamidomethylation of cysteines was defined as fixed modification. Peptide and protein false discovery rates were set to 1% using the target and decoy approach of Maxquant with a forward reverse concatenated database search. Label-free protein quantification was based on at least one unique peptide. All samples were searched together using separate protein LFQ calculation for the different cell lines.

Perseus version 1.6.14<sup>30</sup> was used for further statistical analysis. Protein LFQ intensities were log<sub>2</sub> transformed and a two-sided Student's *t*-test was applied to identify proteins with a significantly changed protein abundance. Additionally, a permutation-based false discovery rate correction for multiple hypotheses was used applying default settings ( $p = .05$ ;  $s_0 = 0.1$ ).<sup>31</sup> For protein categorization, the UniProt subcellular information (download: 2023-05-16) for several organelles and membrane topology was added to the tables.

For the identification of naturally short transmembrane proteins with a type 1 or 3 orientation and short ectodomains of less or equal 75 amino acids, we used additional information from Uniprot including signal peptides, pro peptides, transmembrane domains as well as other topologic domains. All proteins with an annotated single-pass transmembrane domain but unknown topology were categorized as type 1/3 if the extracellular/luminal domain was located N-terminal and C-terminal at cytosol. Single-pass transmembrane proteins with an annotated signal peptide or an annotated N-glycosylation site N-terminally of the TM domain were also defined as type 1/3. Mitochondrial proteins were excluded since  $\gamma$ -secretase is not localized in mitochondria. The ECD length was calculated, as the amino acids N-terminal of the transmembrane domain subtracting known signal and pro peptides. Finally, 157 proteins fulfilled the set thresholds.

## 2.8 | Mass-tag labeling with PEG

Mass-tag labeling to determine protein S-fatty acylation was performed following a similar protocol as previously

described by Percher et al.<sup>32</sup> Briefly, transfected cells were lysed in 500  $\mu$ L of lysis buffer (2.5% [wt/vol] SDS, 100 mM Hepes, 1 mM EDTA pH 7.5) with 13 mM freshly added Maleimide (Sigma) and subsequently sonicated briefly. To block free cysteine thiols, a 4-h incubation at 40°C was carried out, followed by removal of excess unreacted maleimide through acetone precipitation. The resulting pellet was resolubilized in 600  $\mu$ L of binding buffer (1% [wt/vol] SDS, 100 mM Hepes, 1 mM EDTA pH 7.5) at 40°C with continuous shaking. The reaction was divided into three conditions (200  $\mu$ L each). The first condition remained untreated, the second condition received 200 mM NaCl, and the third condition received 200 mM hydroxylamine sulfate (Sigma). Samples were incubated at 37°C for 1 h to release palmitoylated cysteines. Each condition was desalted using pre-equilibrated Zeba Spin desalting columns (7 kDa cutoff, Thermo Fisher 89882), and the second and third conditions were immediately treated with 2 mM 10 kDa PEG maleimide (Sigma 63187). After a 1-hour incubation at 37°C, 30  $\mu$ L of 4X Laemmli buffer (containing 100 mM DTT) was added, and the reaction was stopped at 60°C for 10 minutes. Samples were separated on 4%–20% gradient SDS-PAGE gels (Bio-Rad Laboratories) and blotted against HA.11 and Calnexin (rabbit anti-calnexin [Enzo, Cat ADI-SPA-860]) as described above.

## 2.9 | Flow cytometry

HEK293 cells were seeded and transfected as described above. After overnight incubation with the transfection solution, the cells were washed with 1 $\times$  PBS and supplemented with 500  $\mu$ L of fresh media. Following 48 hours of transfection, the cells were detached using EDTA treatment and subsequently incubated with Alexa Fluor 488-conjugated HA.11 antibody (BioLegend 901509), which specifically targets the extracellular domain of the constructs. An isotype-matching control antibody (BioLegend 400129) was used as a negative control. Flow cytometry analysis was performed using a BD FACS Melody instrument equipped with a bandpass filter of (527  $\pm$  32) nm, and the acquired data were analyzed using FlowJo v10.4.1 software (BD Life Sciences). A total of 100 000 events were acquired for each sample, while debris, cell aggregates, and dead cells were excluded based on forward and side scatter plots, as well as Propidium iodide (Sigma) staining, respectively.<sup>13</sup>

## 2.10 | Statistics and graphics

Statistical tests utilized in the analyses are indicated in the figure legend. GraphPad 9 software was employed

for statistical calculations. Data represent biological replicates. Schematic overviews were created with BioRender.com.

## 3 | RESULTS

### 3.1 | Identification of naturally short substrates and nonsubstrates of $\gamma$ -secretase

To identify potential substrates and nonsubstrates for  $\gamma$ -secretase, we focused on proteins that have a transmembrane domain of type I orientation and additionally a naturally short ectodomain of  $\leq$ 75 amino acids in length. The naturally short substrates do not require ectodomain shedding prior to  $\gamma$ -secretase cleavage. Thus, upon pharmacological inhibition of  $\gamma$ -secretase, the full-length protein form of a naturally short substrate is expected to be enriched in the lysate or membrane fraction of cultured cell lines, similar to the known  $\gamma$ -secretase substrates BCMA and FN14,<sup>21,23</sup> which also have short ectodomains. In contrast, the classical  $\gamma$ -secretase substrates with long ectodomains, such as APP, are not directly cleaved by  $\gamma$ -secretase, but require prior ectodomain shedding, which generates a C-terminal fragment that is the direct  $\gamma$ -secretase substrate. As a consequence, inhibition of  $\gamma$ -secretase does not increase abundance of the full-length substrates, but only of the C-terminal fragments. Yet, given the low abundance of C-terminal fragments, they are difficult to detect in the presence of full-length protein precursors, as both are digested by trypsin during proteomic sample preparation. Consequently, it is challenging to distinguish whether a tryptic peptide is derived from the full-length protein form or from the C-terminal fragment.

To identify naturally short substrates and nonsubstrates of  $\gamma$ -secretase, we used four human cell lines of different tissue origins, breast cancer MCF7 cells, cervix carcinoma HeLa cells, T cell leukemia Jurkat cells and lymphoma U937 macrophage-like cells. The cell lines were treated overnight with the established  $\gamma$ -secretase inhibitor DAPT<sup>33</sup> or DMSO as a control. The proteomes of membrane fractions were determined by nano-liquid chromatography–tandem mass spectrometry. Protein quantification was achieved using label-free quantification and is displayed in volcano plots as the ratio of the protein abundance in the DAPT versus the control DMSO condition (Figure 1, Table S1). Among these proteins, we focused on proteins annotated as type I (with a signal peptide) or type III (without a signal peptide) transmembrane proteins in Uniprot and having an annotated short ectodomain length of up to 75 amino acids, because these may be potential substrates and nonsubstrates for  $\gamma$ -secretase.

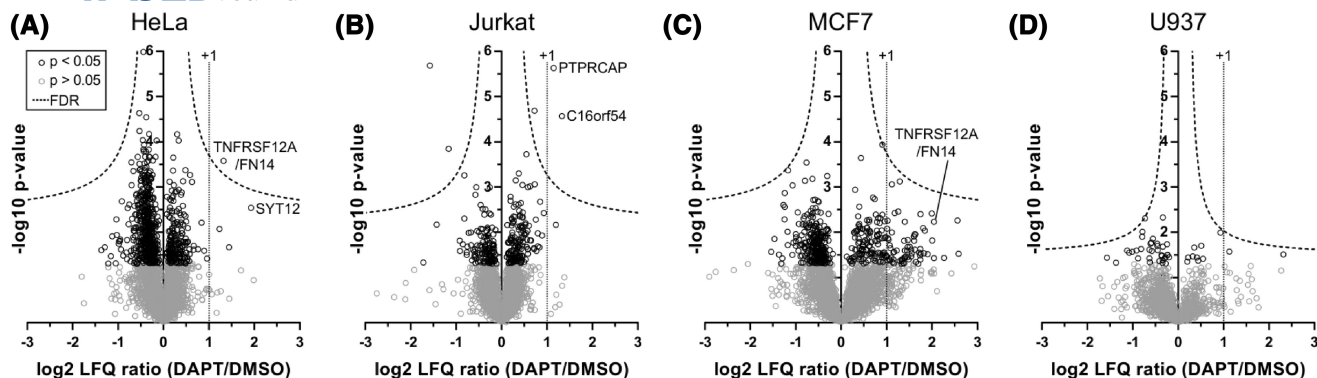


**FIGURE 1** Volcano plots of  $\gamma$ -secretase inhibitor-treated cell lines. Membrane fractions of HeLa (4 DAPT vs 5 DMSO) (A), Jurkat (6 DAPT vs 5 DMSO) (B), MCF7 (5 DAPT vs 5 DMSO) (C) and U937 (4 DAPT vs 5 DMSO) (D) cells were analyzed using mass spectrometry-based proteomics. The  $-\log_{10}$  transformed  $p$ -values (two-sided Student's  $t$ -test) are plotted against the average  $\log_2$  transformed LFQ ratios for each relatively quantified protein. Proteins with a  $p$ -value  $>.05$  are indicated as gray circles, whereas proteins with a  $p$ -value  $<.05$  are displayed as black circles. The dashed hyperbolic curves are the FDR thresholds correcting for multiple hypotheses ( $p = .05$ ,  $s_0 = 0.1$ ).<sup>30,31</sup> Selected single-pass transmembrane proteins with a FDR-significant fold-change  $>1$  (vertical line) are labeled with their gene names.

Adding additional proteins according to UniProt information on signal peptides and topological domains (as described in the methods section) resulted in a total of 157 naturally short membrane proteins, from which we identified 73 proteins and relatively quantified 68 proteins compared to the DMSO control condition (Table S2). Proteins were considered as naturally short substrate candidates for  $\gamma$ -secretase, if their protein abundance was increased by at least two-fold ( $>1.0$  on the  $\log_2$  scale of the  $x$ -axis) and if the change was statistically significant after FDR-correction for multiple hypothesis testing, i.e. if the proteins were above the hyperbolic FDR curves in the volcano plots (Figure 1A–D and Table S1 for proteomic data). In HeLa cells, this yielded TNFRSF12A (better known as FN14), which is a known  $\gamma$ -secretase substrate<sup>23</sup> and validates the screening approach. Additional hits were PTPRCAP and C16orf54 in Jurkat cells, which have been little described to date. C16orf54 has an annotated N-glycosylation site N-terminal of its transmembrane domain, an extracellular domain length of 31 amino acids and is considered as a new naturally short  $\gamma$ -secretase substrate. PTPRCAP was not included in our initial list of 157 transmembrane proteins with short ectodomains (Table S2), because it is annotated in Uniprot simply as a single-pass membrane protein without information of it being a type I or II membrane protein. However, based on the topology prediction of the Phobius webserver,<sup>34</sup> PTPRCAP is annotated as a type I transmembrane protein with a signal peptide of 20 amino acids and an extracellular domain of 15 amino acids. Therefore, we consider it as an additional naturally short  $\gamma$ -secretase substrate candidate. In MCF7 cells, FN14 was strongly enriched by 4.1-fold, but this increase did not reach significance upon FDR correction. Syt12 (quantified in HeLa cells) may be an additional naturally short substrate, because its

increase was 4-fold and was close to reaching significance after FDR correction (Figure 1A).

As we were particularly interested in identifying naturally short nonsubstrate candidates for mechanistic studies, we had a closer look at all the type I or III membrane proteins with a short ectodomain that were quantified in at least one of the four cell lines but not significantly changed upon DAPT treatment. Among the 68 membrane proteins quantified in at least one cell line (Table S2), only the above-mentioned proteins FN14, PTPRCAP, and C16orf54 showed clear evidence for being  $\gamma$ -secretase substrate candidates.

### 3.2 | Validation of naturally short nonsubstrates of $\gamma$ -secretase

For validation and further mechanistic analysis, we chose six proteins from the 68 apparent nonsubstrate candidates that differed in the length of their ectodomain and were consistently detected in at least one cell line. FXYD domain-containing ion transport regulator 3 (FXYD3) has a very short ectodomain of 18 amino acids. FXYD6, which has an ectodomain of 17 amino acids, does not have a pronounced sequence similarity to FXYD3 and was included as a comparison to FXYD3. The ectodomain lengths of LYRIC, PMEPA1 and PTTG1IP are 49, 41 and 64 amino acids, respectively. FXYD3 and FXYD6 are auxiliary subunits of the Na,K-ATPase.<sup>35,36</sup> LYRIC (Metadherin; MTDH), PMEPA1 (TMPEPA1) and PTTG1IP (pituitary tumor-transforming gene binding factor; PBF) have not been studied in much detail, but may modulate multiple signaling pathways and are linked to malignancies.<sup>37–39</sup> We also included SYT12, which has an ectodomain length of 19 amino acids and is a homolog of the previously identified

naturally short  $\gamma$ -secretase substrate SYT7.<sup>22</sup> For SYT12, it remained possible from the proteomics experiment that it may be cleaved by  $\gamma$ -secretase, even though its changes in HeLa cells had not reached significance (Figure 1A).

To validate the nonsubstrate candidates, we transiently transfected human embryonic kidney 293 (HEK293) cells with plasmids encoding the nonsubstrate candidates. As a positive control for a substrate, we included FN14.<sup>23</sup> As a positive control for a nonsubstrate, we included a C-terminal fragment of integrin  $\beta$ 1 (ITGB1) carrying 25 amino acids of

its natural ectodomain, which was previously established as a nonsubstrate.<sup>24</sup> All proteins carried an N-terminal HA-epitope tag and a C-terminal double FLAG-epitope tag (Figure 2A for a scheme). Cells were incubated overnight either with DAPT or DMSO as a control. The full-length proteins were detected in the cell lysate with an anti-HA-tag antibody. In contrast to the endogenously expressed short proteins, where DAPT increased protein abundance of FN14 in the proteomic experiment (Figure 1A), this increase was not seen upon overexpression of FN14 (Figure 2B), in line

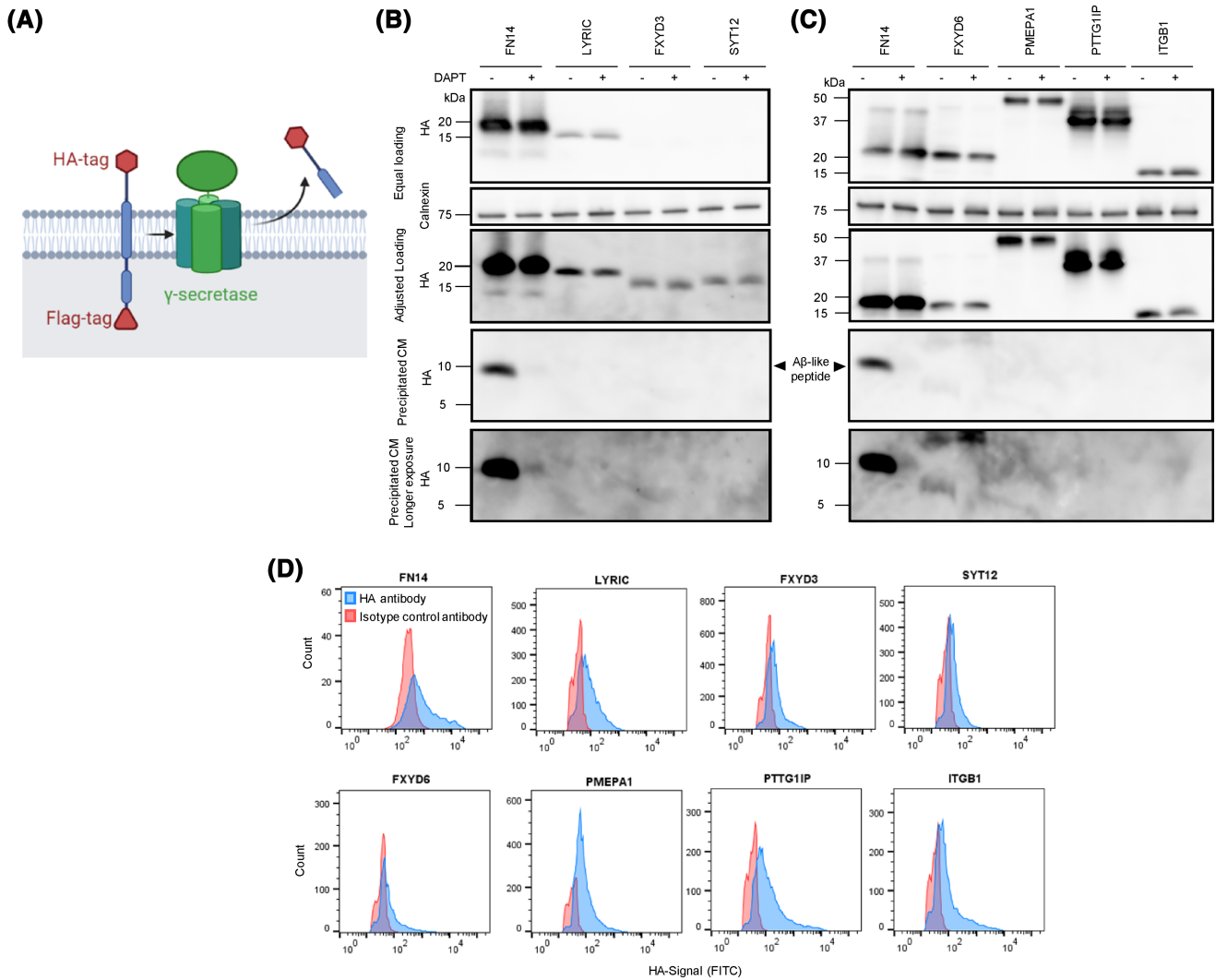


**FIGURE 2** Validation of naturally short nonsubstrates of  $\gamma$ -secretase. (A) Schematic overview of the construct design, where the type I orientated proteins with a naturally short ectodomain were tagged with a N-terminal HA-tag (hexagon) and a double C-terminal FLAG-tag (triangle). Intramembrane proteolysis by  $\gamma$ -secretase would result in the secretion of a HA-tagged fragment into the conditioned medium. (B and C) Lysates of HEK293 cells transfected with putative (non)-substrates of  $\gamma$ -secretase were loaded next to each other according to protein amount (Equal amounts, top two panels). Next, loading was adjusted according to band intensity in order to better visualize the constructs (third panel from the top). The generation of a  $\gamma$ -secretase cleavage product was measured by immunoprecipitating the conditioned medium (CM) with an anti-HA-tag antibody and loading volumes of the precipitate corresponding to the adjusted lysates. The generation of the  $A\beta$ -like cleavage product of FN14 is indicated by a black arrowhead and was detected upon blotting with anti-HA antibody. Representative blots from  $N = 3$  experiments are presented. (D) In order to assess surface abundance of the putative (non)-substrates, HEK293 cells were transfected with the described constructs and analyzed by flow cytometry. Cells were labeled with HA antibody (blue) to the N-terminal HA-tag of the constructs, or isotype control (red). Shown are representative histograms from  $N = 2$  experiments.

with our previous study.<sup>23</sup> Presumably, the transfected protein is much more abundant than the endogenous protein so only a small fraction is processed by  $\gamma$ -secretase during the experiment. The full-length proteins were detected with various abundance when the same amounts of total lysate protein were loaded (Figure 2B,C, top two panels). Thus, the proteins were additionally loaded on a separate gel with varying protein amounts to better visualize that all proteins were expressed (Figure 2B,C, third panel from the top).

Among the two substrate cleavage products generated by  $\gamma$ -secretase, the ICDs are short-lived and often difficult to detect. Thus, we used the secretion of the small N-terminal A $\beta$ -like peptide into the conditioned medium as a criterion to classify a protein as a substrate or a nonsubstrate. Given the low expression level of some constructs, the secreted peptide was immunoprecipitated with an HA-tag antibody. As expected for the positive control, DAPT strongly reduced the secreted FN14 peptide in the conditioned medium for the  $\gamma$ -secretase substrate FN14 (Figure 2B,C), while no secreted peptide was detected for the known nonsubstrate ITGB1, neither under control (DMSO) nor DAPT treatment conditions (Figure 2C). Likewise, no secreted peptide was detected for LYRIC, FXYD3, SYT12, PMEPA1 and PTTG1IP (Figure 2B,C), whereas for FXYD6 a shade of a low-intensity band of ~7kDa was seen that appeared reduced with DAPT, indicating that FXYD6 may potentially be cleaved by  $\gamma$ -secretase. We conclude that these six proteins are either nonsubstrates or cleaved with low efficiency, which is in line with the proteomic result that the abundance of these proteins – even at endogenous expression – was not significantly increased upon DAPT treatment in the membrane fraction of the cultured cells (Figure 1).

$\gamma$ -Secretase cleaves its substrates at the plasma membrane and in the endocytic pathway. To ensure that the overexpressed proteins would traffic through the secretory pathway, we used flow cytometry to verify that all expressed proteins were detected at the cell surface with an anti-HA-tag antibody, as compared to an isotype control antibody (Figure 2D).

We conclude that, compared to FN14, the membrane proteins FXYD3, FXYD6, LYRIC, PMEPA1, PTTG1IP and SYT12, which all have short ectodomains, are either cleaved with low efficiency or not at all by  $\gamma$ -secretase. Thus, we considered them as nonsubstrates for the subsequent mechanistic study.

### 3.3 | The transmembrane domain sequence determines the cleavage efficiency of substrates

Because  $\gamma$ -secretase cleaves its substrates within their TMD, we asked whether the transmembrane sequence of the

nonsubstrates is a determinant that prevents their cleavage. To exclude effects from sequences in the ectodomain or cytoplasmic domain, we used the validated naturally short substrate FN14<sup>23</sup> as a model substrate and replaced only its TMD with the ones from the validated nonsubstrate proteins (Figure 3A). These FN14 TMD swap constructs were transiently transfected into HEK293 cells. We also included the TMDs of three known  $\gamma$ -secretase substrates with long ectodomains – APP, Notch1, CACHD1<sup>40</sup> – to be able to compare the cleavage efficiencies of the nonsubstrate TMDs to some known substrate TMDs. As negative controls we included the TMDs of the nonsubstrate ITGB1 and a synthetic TMD consisting of 21 leucines (poly leucine 21, pL21, same number of amino acids as in the FN14 TMD), which has a strongly reduced conformational flexibility and prevents  $\gamma$ -secretase cleavage, as shown for the substrate C99.<sup>13</sup>

Full-length proteins in the lysate and the secreted peptides in the conditioned medium were detected on the same membrane by immunoblot using an anti-HA antibody. Immunoblot intensity of the secreted peptides were quantified and normalized to the intensity of the corresponding full-length protein to control for potential differences in transfection efficiency or protein expression. This ratio (secreted peptide/full-length protein) was taken as a measure of cleavage efficiency of the protein by  $\gamma$ -secretase and was set to 1 for wild-type FN14, for which the secreted peptide and the full-length protein were well detectable (Figure 3B). Cleavage efficiencies for the distinct TMD swap constructs in the FN14 backbone varied by up to 200-fold between FN14 with the TMD of FXYD3 versus PMEPA1 (Figure 3B, and quantification in 3C [logarithmic scale]). The positive and negative controls showed the expected cleavage efficiencies. Specifically, the FN14 constructs with the TMDs of the known  $\gamma$ -secretase substrates Notch1, CACHD1 and APP were more efficiently cleaved by  $\gamma$ -secretase than the reference construct with the FN14 TMD. As expected for the negative control, FN14 with the synthetic pL21 TMD was barely cleaved and showed the lowest cleavage efficiency of all constructs tested. FN14 with the TMD of the nonsubstrate ITGB1 yielded little of the secreted peptide and showed a low cleavage efficiency compared to the reference construct with the FN14 TMD, consistent with ITGB1 being a nonsubstrate for  $\gamma$ -secretase. Among the TMDs of our newly identified nonsubstrates or low-efficient substrates for  $\gamma$ -secretase (FXYD3, SYT12, LYRIC, FXYD6, PTTG1IP, PMEPA1), some behaved similar to ITGB1 and showed a much lower cleavage efficiency (FXYD6, PTTG1IP, PMEPA1) than the reference FN14, whereas others were more efficiently cleaved by  $\gamma$ -secretase (FXYD3, SYT12, LYRIC) than FN14. All proteins were efficiently expressed at the surface of the transfected HEK293 cells, as seen by flow cytometry (Figure S1). Together, these experiments



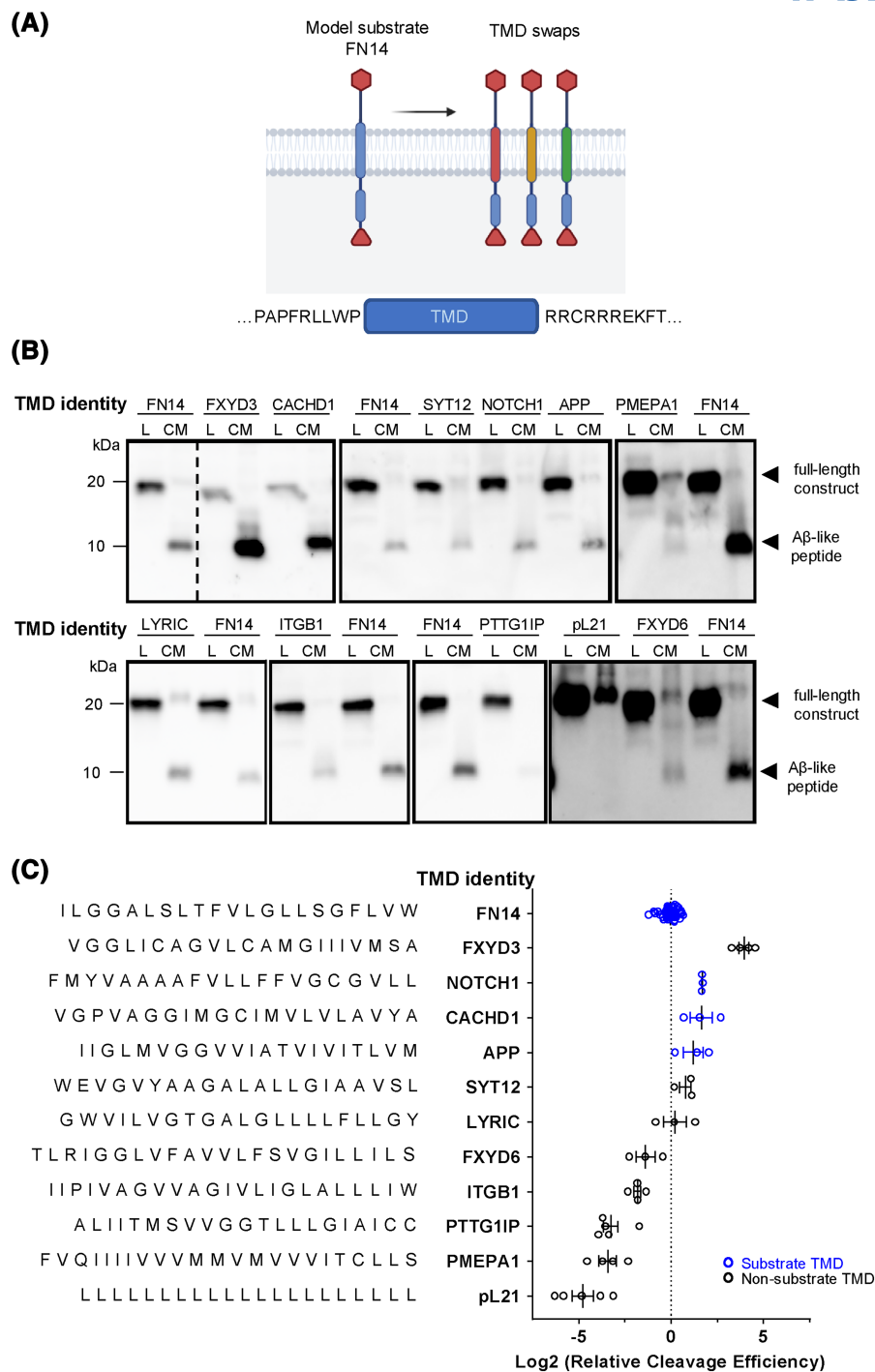


**FIGURE 3** Transmembrane domains of putative nonsubstrates are cleavable when swapped into the backbone of the substrate FN14. (A) The schematic overview shows the construct design, where the FN14 construct serves as the backbone with an N-terminal HA-tag (hexagon) and a C-terminal double FLAG-tag (triangle). Transmembrane domains (TMDs) of known substrates and putative nonsubstrates were swapped into the model substrate FN14 backbone. The 10 juxtamembrane amino acids of the FN14 backbone are depicted. (B) Conditioned medium (CM) and lysates (L) of HEK293 cells transfected with FN14 constructs carrying the indicated transmembrane domains (TMD) were loaded next to each other. The generation of an A $\beta$ -like cleavage product (soluble FN14 or mutants thereof) is indicated by a black arrowhead and was detected upon blotting with anti-HA antibody. Representative blots from  $N=3-5$  experiments are presented. For FN14, which served as the reference,  $N=42$ . A dashed line indicates that the samples were run on the same gel, but not directly next to each other. (C) The amino acid sequence of each transmembrane domain is provided alongside the logarithmic cleavage efficiency of the respective TMD swap construct. The relative cleavage efficiency is defined as the intensity ratio of the A $\beta$ -like peptide (soluble FN14 or mutants thereof) at approximately 10kDa in the conditioned media to the full-length protein at approximately 20kDa in the cell lysate, normalized to the wild-type FN14 construct (Quantification of B). All quantification data are shown as mean  $\pm$  SEM and each dot represents one biological replicate  $N=3-5$ . For FN14, which served as the reference,  $N=42$  were quantified. Transmembrane domains of proteins identified as substrates are highlighted in blue.

demonstrate that the TMDs of several nonsubstrates can be efficiently cleaved by  $\gamma$ -secretase if present within the backbone of a well-cleaved  $\gamma$ -secretase substrate. We conclude that a cleavable TMD is required for cleavage by  $\gamma$ -secretase but that the backbone, i.e. domains outside of the TMD, such as the N-terminal ectodomain or the C-terminal cytoplasmic domain, may prevent efficient cleavage by  $\gamma$ -secretase.

### 3.4 | The C-terminal half of the transmembrane domain determines the cleavage efficiency

$\gamma$ -Secretase cleaves its substrates typically first at the C-terminal end of their TMD and then proceeds in a step-wise manner towards the middle of the TMD, thereby shortening the N-terminal cleavage product until it is short enough to slip out of the membrane. To narrow down which part of the TMDs investigated in our study may be relevant in determining the cleavage efficiency, we focused on the TMDs of FN14 (used as reference), FXYD3 (very efficiently cleaved) and PTTG1IP (poorly cleaved, Figure 3C) and exchanged among them either the N- or the C-terminal half of their TMDs. As in those experiments above where complete TMDs were exchanged (Figure 3), epitope-tagged domains of FN14 provided the extracellular and cytoplasmic sequences of these constructs (Figure 4A for a scheme). Constructs with the C-terminal TMD half of FN14 showed a cleavage efficiency similar to the entire FN14 TMD (Figure 4B, quantification in C). In contrast, constructs with the N-terminal TMD half of FN14 showed the cleavage efficiency of the corresponding protein (FXYD3, PTTG1IP) from which the C-terminal TMD half was taken. Likewise, the chimeric constructs with half TMDs from FXYD3 and PTTG1IP showed the cleavage efficiency of the TMD from which the C-terminal TMD half was taken. We conclude that the C-terminal half of the TMDs has a major influence on the cleavage efficiency of the constructs used in our assay and that the PTTG1IP TMD strongly suppresses cleavage by  $\gamma$ -secretase.

### 3.5 | Substrate palmitoylation interferes with substrate cleavage

Comparison of the C-terminal TMD ends in Figure 4C (PTTG1IP, FXYD3 and FN14) revealed the presence of a double cysteine motif at the C-terminal TMD end of PTTG1IP, which is not found in FXYD3 and FN14 and not in the other proteins tested in Figure 3. Because such cysteine motifs may be modified post-translationally with

the fatty acid palmitic acid,<sup>41</sup> we considered that such palmitoylation may potentially interfere with  $\gamma$ -secretase cleavage. Thus, we tested whether pharmacological inhibition of palmitoylation with 2-bromopalmitic acid (2-BP) or exchange of both cysteines to serines would increase  $\gamma$ -secretase cleavage of the FN14 mutant with the PTTG1IP TMD (Figure 5A). In fact, 2-BP enhanced cleavage of FN14 with the PTTG1IP TMD, whereas it had no effect on FN14 with its wild-type TMD, used as a control (Figure 5B,C). This suggests that the TMD of PTTG1IP, but not of FN14, is palmitoylated and that inhibition of palmitoylation enhances cleavage by  $\gamma$ -secretase. A similar result was obtained when membranes from the transfected HEK293 cells were subject to an *in vitro*  $\gamma$ -secretase assay, in which the second cleavage product by  $\gamma$ -secretase – the ICD –, can be detected for FN14, in agreement with our previous publication<sup>23</sup> (Figure S2). 2-BP enhanced ICD abundance for FN14 with the PTTG1IP TMD, whereas it had no effect on FN14 with its wild-type TMD, that was used as a negative control (Figure S2). We also included wild-type, full-length PTTG1IP, but did not detect its ICD, not even after 2-BP treatment (Figure S2). Potentially, its ICD was below the detection limit of our immunoblot even upon 2-BP treatment. Alternatively, inhibition of palmitoylation by 2-BP may not be sufficient for cleavage of PTTG1IP by  $\gamma$ -secretase, as the N-terminal extracellular domain and the C-terminal intracellular domains of PTTG1IP may additionally prevent binding to or cleavage by  $\gamma$ -secretase.

Next, we replaced both cysteines within the PTTG1IP TMD in the FN14 backbone by serines, which are structurally similar to cysteines but cannot be palmitoylated. This mutant PTTG1IP-SS also enhanced cleavage and did so even more strongly than 2-BP. As expected, 2-BP did not further enhance cleavage of FN14 with the PTTG1IP-SS TMD, because this mutant cannot be palmitoylated within its TMD. We also generated two additional nonpalmitoylatable variants of FN14 with the PTTG1IP TMD, in which the two cysteines were replaced by the hydrophobic amino acids alanine-alanine (AA) or alanine-leucine (AL) (Figure S3A). Similar to FN14 with the PTTG1IP-SS TMD, both the PTTG1IP-AA and the PTTG1IP-AL TMD variants strongly increased cleavage by  $\gamma$ -secretase (Figure S3A).

To further demonstrate the relevance of the two cysteine residues, we introduced them at the C-terminal TMD end of the very well-cleaved substrate FN14 with the FXYD3 TMD. Introduction of the cysteines nearly completely blocked cleavage by  $\gamma$ -secretase. As a control, addition of 2-BP enhanced cleavage of this mutant protein to an extent similar to what was seen for FN14 with the PTTG1IP TMD upon 2-BP treatment (Figure 5B,C). In a control experiment, the mutations still allowed surface expression of the proteins in transfected HEK293 cells (Figure S3B). As a further control, we also included the

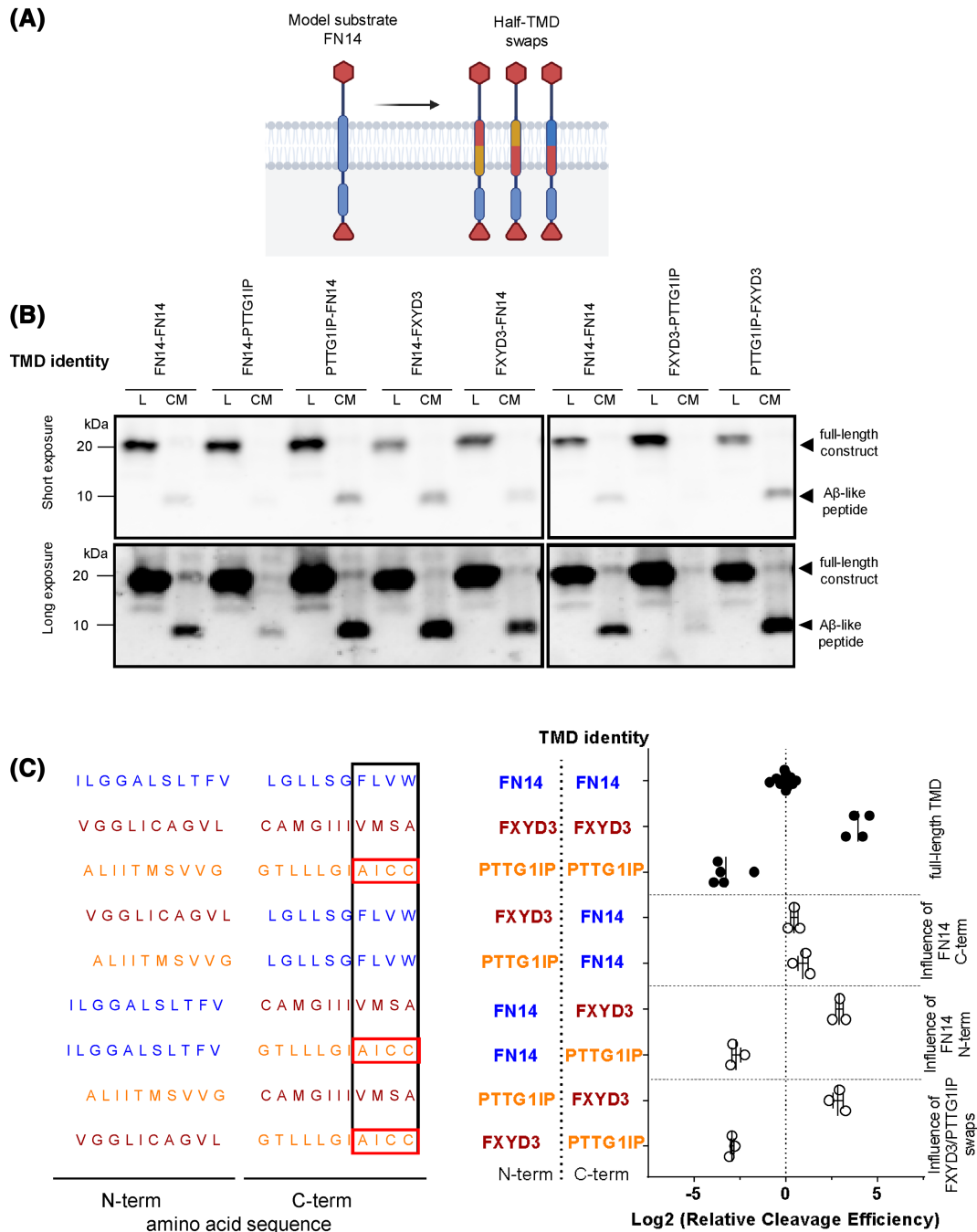


**FIGURE 4** Cleavage of half-TMD swap FN14 constructs by  $\gamma$ -secretase. (A) The schematic overview shows the construct design, where the FN14 construct serves as the backbone with an N-terminal HA-tag (hexagon) and a C-terminal double FLAG-tag (triangle). To elucidate which part of the TMD predominantly affects cleavage by  $\gamma$ -secretase, the N- and C-terminal halves of the TMDs of the nonsubstrates FXYD3 and PTTG1IP were inserted into the corresponding positions within the TMD of the model substrate FN14. For example, FN14-PTTG1IP refers to a construct consisting of the N-terminal half of the FN14TMD fused to the C-terminal half of the PTTG1IP TMD. (B) Conditioned medium (CM) and lysates (L) of HEK293 cells transfected with FN14 constructs carrying the indicated half-transmembrane domains (TMD) were loaded next to each other. The generation of an A $\beta$ -like cleavage product (soluble FN14 or mutants thereof) is indicated by a black arrowhead and was detected upon blotting with anti-HA antibody. Representative blots from  $N=3$  experiments are presented. For FN14, which served as the reference,  $N=12$  were tested. (C) The amino acid sequence of each transmembrane domain is provided alongside the logarithmic cleavage efficiency of the respective construct. The boxes highlight the four most C-terminal amino acids of the transmembrane domain, as annotated by Uniprot, where the initial cleavage by  $\gamma$ -secretase typically occurs. The sequences with the double cysteine motif are additionally highlighted with a red box. The relative cleavage efficiency, defined as the intensity ratio of the A $\beta$ -like peptide (soluble FN14 or mutants thereof) at approximately 10kDa in the conditioned media to the full-length protein at approximately 20kDa in the cell lysate, normalized to FN14, is depicted (Quantification of B). Values for the constructs with the entire TMD of FXYD3 or PTTG1IP were taken from Figure 3C. All quantification data are shown as mean  $\pm$  SEM and each dot represents one biological replicate  $N=3$ . For FN14, which served as the reference,  $N=12$  were quantified.

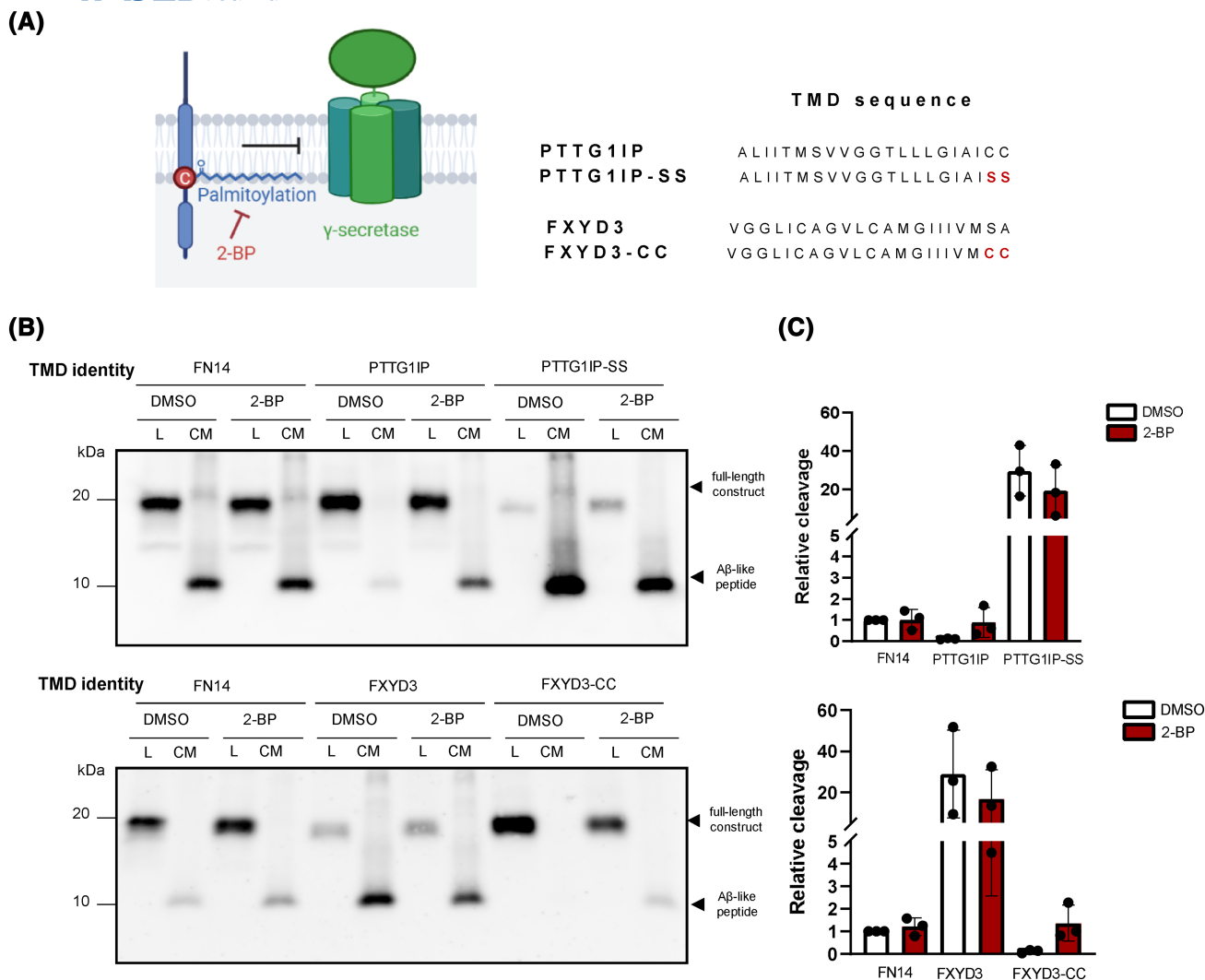


**FIGURE 5** Inhibitory effect of substrate palmitoylation on substrate cleavage. (A) Schematic overview of a construct carrying a C-terminal cysteine in the TMD, which is palmitoylated. This posttranslational modification may interfere with normal cleavage of the TMD by  $\gamma$ -secretase. The covalent attachment of the palmitic acid to cysteines can be prevented with the general protein palmitoylation inhibitor 2-bromopalmitate (2-BP). The right part of the panel gives an overview of the TMD sequences of the indicated constructs carrying the wild-type or mutated (red) TMD sequence. (B) Conditioned media (CM) and lysates (L) of HEK293 cells transfected with FN14 constructs carrying the indicated transmembrane domains (TMD) were loaded next to each other. The detection of an A $\beta$ -like cleavage product (indicated by a black arrowhead, soluble FN14 or mutants thereof) is evident in the CM of HEK293 cells transfected with the TMD constructs as validated through blotting with the anti-HA antibody. Cells were treated either with DMSO as a control or the palmitoylation inhibitor 2-BP. Representative blots from  $N=3$  experiments are presented. (C) The relative cleavage efficiency, defined as the intensity ratio of the A $\beta$ -like peptide to the full-length protein normalized to FN14 (which is set to 1), is depicted (quantification of B). All quantification data are shown as mean  $\pm$  SEM. Each dot represents one biological replicate  $N=3$ .

two cysteines at the C-terminal TMD end of the well-cleaved substrate FN14 with the TMD of APP. Similar to FN14 with the FXDYD3 TMD, the two cysteines nearly completely blocked cleavage by  $\gamma$ -secretase, whereas addition of 2-BP enhanced cleavage of this mutant protein to an extent similar to what is seen for FN14 with the PTTG1IP TMD upon 2-BP treatment (Figure S4).

We conclude that in the constructs tested, a palmitoylation motif at the cytoplasmic end of the PTTG1IP or FXDYD3 or APP TMD is sufficient to block cleavage by

$\gamma$ -secretase and that inhibition of palmitoylation is a means to increase cleavage of these constructs by  $\gamma$ -secretase.

To demonstrate physical palmitoylation of FN14 with the PTTG1IP TMD, but not of its variant PTTG1IP-SS in the transfected HEK293 cells, we used an established assay<sup>32</sup> in which the low molecular weight molecule palmitate is replaced by polyethyleneglycol (PEG). Replacing palmitate with the 10 kDa PEG leads to a molecular weight shift that can be detected by immunoblot, as shown previously for calnexin.<sup>32</sup> For the replacement, cell lysates were

treated with hydroxylamine (NH<sub>2</sub>OH), which removes palmitoylation and makes the resulting free cysteine amenable to modification with PEG *in vitro*.

The cytoplasmic domain of FN14, which was used for our domain swap constructs and thus, also of the FN14 chimera with the PTTG1IP TMD, contains naturally two cysteine residues, one of which is just three amino acids downstream of the transmembrane domain (Figure 3A). One or both of these cytoplasmic cysteines in FN14 may potentially be palmitoylated according to the SwissPalm database<sup>42</sup> and could, thus, possibly interfere with detection of palmitoylation within the TMD of FN14-PTTG1IP. To exclude this possibility, we mutated both cysteines in the cytoplasmic domain of FN14 to alanine (Figure 6A) and verified that both cysteine mutations outside of the TMD did not affect the cleavage by  $\gamma$ -secretase of all constructs used for the palmitoylation detection assay (Figure 6B). In the palmitoylation assays, the TMD of FN14 was indeed not palmitoylated, whereas the TMD of PTTG1IP, but not of the PTTG1IP-SS variant, was inferred to be palmitoylated (Figure 6C) based on the molecular weight shift induced by modification with PEG. The extent of the molecular weight increase indicates that only one of the two cysteines in the TMD was palmitoylated. Similar results were obtained for FXYD3, which was palmitoylated only when carrying the di-cysteine palmitoylation motif. As a positive control, calnexin was detected as being palmitoylated in each sample (Figure 6C).

Taken all together, we conclude that palmitoylation within a substrate's TMD can be a mechanism to reduce the extent of substrate cleavage by  $\gamma$ -secretase.

## 4 | DISCUSSION

Our study identified new substrate candidates and putative nonsubstrates for  $\gamma$ -secretase and demonstrates that the TMD sequence of membrane proteins and their palmitoylation are key features for substrate recognition and cleavage efficiency of  $\gamma$ -secretase.

Palmitoylation is a reversible post-translational modification that is found in approximately 10% of the human proteome.<sup>42,43</sup> Protein acyl transferases covalently link the fatty acid palmitic acid to cysteine residues of cytosolic and transmembrane proteins, whereas acyl protein thioesterases can remove this modification.<sup>44</sup> Palmitoylation can affect cellular localization and function of membrane proteins, such as the signaling of surface receptors or the activity of the protease BACE1,<sup>45,46</sup> but in many cases, the exact role of palmitoylation is not yet understood. Palmitoylation of transmembrane proteins occurs within their cytoplasmic domains or even at the cytosolic end of their TMDs. Our study demonstrates that palmitoylation

within a substrate's TMD can block cleavage by  $\gamma$ -secretase. The model substrate FN14 with the TMD of PTTG1IP was only cleaved by  $\gamma$ -secretase when its TMD was not palmitoylated, as shown via pharmacological inhibition of palmitoylation, or when the two cysteine residues at the C-terminal end of the substrate's TMD were replaced by serine, alanine or leucine. Conversely, when this di-cysteine-motif was transferred to the same location within the TMD of the well-cleaved model substrate FN14 containing the FXYD3 or APP TMD, it became palmitoylated, resulting in strongly reduced cleavage by  $\gamma$ -secretase. Because palmitoylation is a reversible post-translational modification, it is conceivable that regulated palmitoylation/depalmitoylation controls  $\gamma$ -secretase cleavage of some substrates, but at present little is known about such cellular processes or stimuli.

We consider different scenarios of how palmitoylation within a TMD may interfere with  $\gamma$ -secretase cleavage of substrates. This modification may sterically hinder the access of the substrate's TMD to the active site of  $\gamma$ -secretase, which accommodates only a single TMD of a substrate, as demonstrated by cryo-electron microscopy for  $\gamma$ -secretase with substrates derived from APP or Notch.<sup>20,47</sup> It is also conceivable that the palmitoylation may retain the substrate's TMD in the lipid environment of the membrane or tilt the TMD and prevent it from entering the protein environment provided by the multiple TMDs of presenilin, the active site-containing subunit of  $\gamma$ -secretase. Additionally, the two cysteines, where palmitoylation occurs in the FN14 substrate with the PTTG1IP TMD, are located exactly at the site where  $\gamma$ -secretase would initially cleave its substrate, so that palmitoylation at this site may interfere with the access of the two catalytic aspartates of  $\gamma$ -secretase to the scissile peptide bond. Finally, the palmitic acid may interfere with the partial unfolding of the substrate's TMD helix at its C-terminal end which appears to be required for the formation of a stable enzyme-substrate complex needed for proteolysis to occur.<sup>20,47</sup>

PTTG1IP is not the only transmembrane protein with a type I-oriented TMD that has a cysteine near the C-terminal end of its TMD. However, not all such cysteines are necessarily palmitoylated or functionally relevant. Among the 149 proteins being reported as  $\gamma$ -secretase substrates,<sup>23</sup> 20 carry a cysteine at the C-terminal end of their TMD (Table S3), where we considered the last four C-terminal amino acids of the TMDs as they are predicted by the TMHMM algorithm.<sup>48</sup> This is the region where the initial cleavage by  $\gamma$ -secretase typically occurs. It is largely unclear whether these proteins are indeed palmitoylated. Eight of these 20 proteins were found to be palmitoylation candidates in palmitoyl-proteomics studies,<sup>42</sup> but only two of them were experimentally verified (CD44 and TNFRSF21). Five additional proteins out of the eight

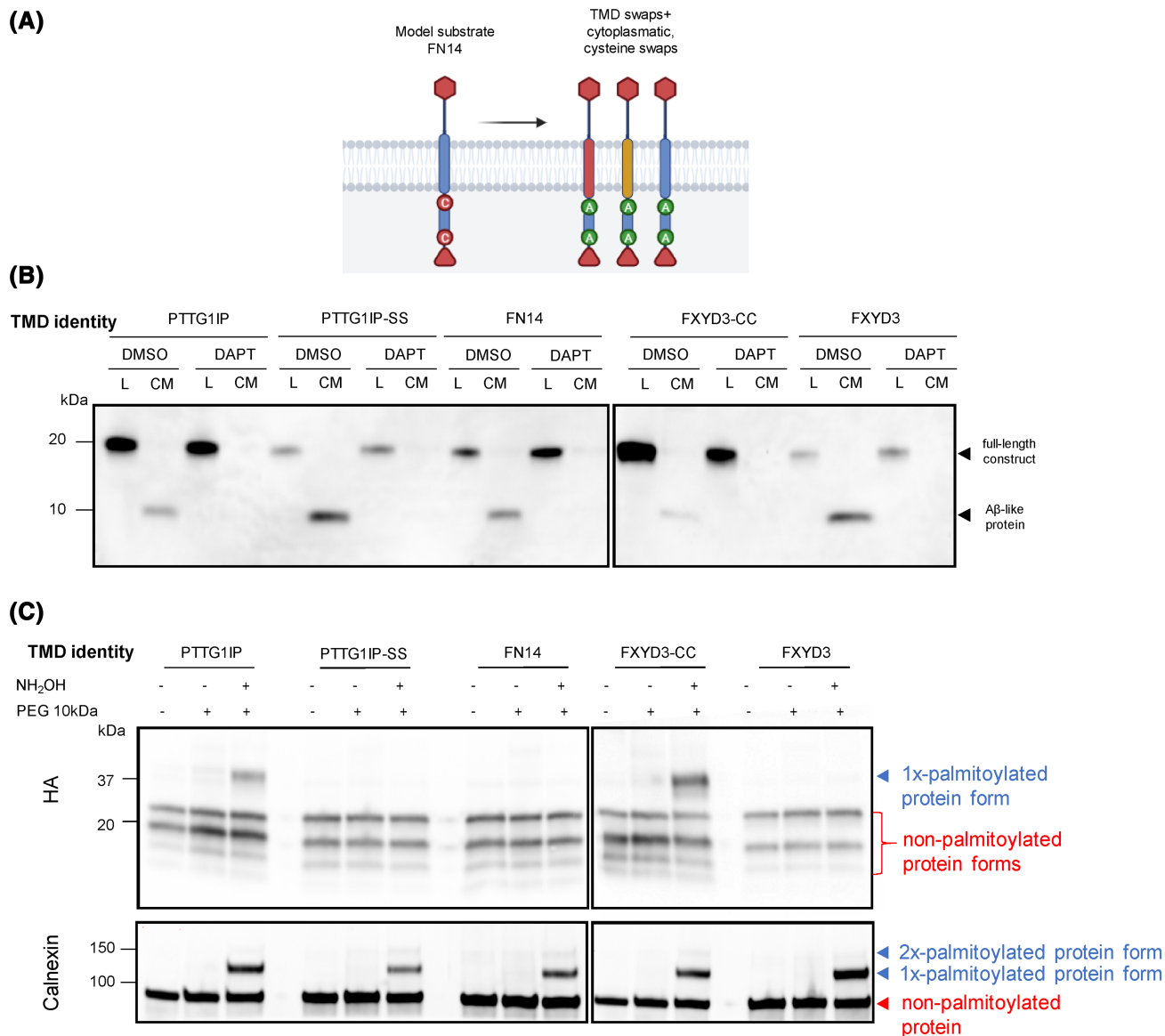


**FIGURE 6** Confirmation of substrate palmitoylation at C-terminal cysteines in the TMD. (A) The schematic overview shows the construct design, where the FN14 construct endogenously carries two cysteines that were exchanged for alanines. Transmembrane domains (TMDs) of FXYD3 and PTTG1IP either carrying the two cysteines within their transmembrane domain or not (see Figure 5A) were swapped into the modified FN14 backbone. (B) Conditioned medium (CM) and lysates (L) of HEK293 cells transfected with FN14 constructs carrying the indicated transmembrane domains (TMD) were loaded next to each other. The detection of an A $\beta$ -like cleavage product (indicated by a black arrowhead) is evident in the CM of HEK293 cells transfected with the TMD constructs as validated through blotting with the anti-HA antibody. Cells were treated either with DMSO as a control or DAPT to validate the  $\gamma$ -secretase-dependent cleavage. Representative blots from  $N=2$  experiments are presented. (C) Detection of PEGylation (inferring palmitoylation) of FN14 constructs (upper panel, HA antibody) and endogenous calnexin (lower panel). Treatment with hydroxylamine (NH<sub>2</sub>OH) removes palmitate. Subsequent addition of a 10 kDa mass label (PEG) to the free cysteine increased the molecular weight, as indicated by a blue arrowhead. In this experimental set-up, nonpalmitoylated constructs ran as several bands for unknown reasons. The lower calnexin blot serves as a quality control for the PEG-labeling approach, confirming the NH<sub>2</sub>OH-dependent PEG-labeling of both cysteines in the TMD of calnexin, as denoted by two blue arrowheads. Representative blots from  $N=3$  experiments are presented.

candidates have cytoplasmic cysteines distant from the TMD. Thus, even if they can be palmitoylated, it remains unclear whether palmitoylation occurs at the TMD boundary, where it may directly influence  $\gamma$ -secretase cleavage, or distant from the membrane, where it might not directly

interfere with  $\gamma$ -secretase cleavage. In principle, palmitoylation at such distant cysteines outside of the TMD may still influence  $\gamma$ -secretase cleavage, but in an indirect manner, as reported previously for the transmembrane proteins betacellulin, p75NTR and the voltage-gated sodium channel

SCN1B.<sup>49–51</sup> In those cases, palmitoylation was required for stability or cell surface transport of the transmembrane protein, so that loss of palmitoylation reduced substrate levels or their trafficking towards  $\gamma$ -secretase. Additionally, it is possible that for some proteins with cysteines in their TMD only a fraction of their molecules is palmitoylated so that enough nonpalmitoylated molecules are available for cleavage by  $\gamma$ -secretase. As a consequence, palmitoylation may not lead to measurable changes in their cleavage by  $\gamma$ -secretase. Interestingly, Aph-1 and nicastrin, two of the four  $\gamma$ -secretase complex subunits, are also palmitoylated.<sup>52</sup> While this modification appears to stabilize the  $\gamma$ -secretase complex, it is not required for  $\gamma$ -secretase activity.

Another result of our study is that a cleavable TMD is required for cleavage by  $\gamma$ -secretase, but that domains outside of the TMD, such as the N-terminal ectodomain or the C-terminal cytoplasmic domain may prevent efficient cleavage by  $\gamma$ -secretase. Several of the membrane proteins with short ectodomains, i.e., FXYD3, FXYD6, LYRIC, PMEPA1, PTTG1IP, SYT12, were found to not be efficiently cleaved by  $\gamma$ -secretase in their wild-type forms, as monitored by (a) the lack of the endogenous proteins being enriched upon  $\gamma$ -secretase inhibition using mass spectrometry and (b) by the lack of secretion of an A $\beta$ -like peptide upon protein overexpression. Yet, in the domain swap experiments, the TMDs of the nonsubstrates FXYD3, LYRIC and SYT12 were efficiently cleaved by  $\gamma$ -secretase when flanked by the extracellular and cytoplasmic domains of the well-cleaved  $\gamma$ -secretase substrate FN14. A central role for a domain other than the TMD in recognition by  $\gamma$ -secretase is in line with previous data revealing that the initial interaction between a substrate and  $\gamma$ -secretase involves a substrate's ectodomain.<sup>53</sup>

Our study also highlights that a substrate's TMD sequence – even in the absence of palmitoylation – determines the efficiency with which it is cleaved and processed to the secreted A $\beta$ -like peptide relative to the amount of full-length substrate in the lysate. Using FN14 as the protein backbone, the cleavage efficiency differed by up to 200-fold between the most (FXYD3) and the least (pL21) efficiently cleaved TMD. Similarly, previous studies demonstrated that point mutations in the TMD of the APP-derived substrate C99 can affect total A $\beta$  generation via decreasing the efficiency of  $\gamma$ -secretase cleavage and/or processing of long A $\beta$  to shorter A $\beta$  species.<sup>54–60</sup> While the mechanism underlying these differences in cleavability is not fully clear, it is possible that the sequence of the C-terminal TMD halves – which showed the strongest effect on cleavage efficiency in our study – differs structurally in its ability and affinity to bind to the active site of  $\gamma$ -secretase, thus allowing more or less efficient cleavage. Alternatively, the sequences of the C-terminal TMD halves may differ in their ability to unfold and form a  $\beta$ -sheet that is required for the formation of a stable enzyme-substrate

complex needed for proteolysis to occur.<sup>20,47</sup> Additionally, a combined experimental approach using cleavage assays, mutagenesis, deuterium-hydrogen exchange analysis and NMR spectroscopy recently uncovered three crucial domains within APP and Notch TMD helices.<sup>13,61,62</sup> A conformationally flexible N-terminal domain may facilitate the passage of the TMD from a bilayer towards the catalytic aspartates of presenilin, the enzymatic subunit of  $\gamma$ -secretase. In addition, flexibility may enhance presentation of a C-terminal TMD domain to presenilin domains, with whom it forms a  $\beta$ -sheet stabilizing the unfolded cleavage-competent state. In the unfolded state, that domain of the TMD encompassing the initial cleavage site is likely to tightly dock into the catalytic cleft of presenilin.

Given the wide range of cleavage efficiencies in our study, it appears possible that any TMD sequence may be cleaved and processed to some extent by  $\gamma$ -secretase, provided that it is in a type I orientation – which is required for any  $\gamma$ -secretase substrate – and that it has permissive extracellular and cytoplasmic domains. However, for some TMDs the cleavage efficiency may be so low – as for example for FN14-PTTG1IP in our study – that they may effectively be considered as nonsubstrates of  $\gamma$ -secretase.

In summary, our study provides new insights into the mechanisms that control substrate recognition and cleavage efficiency by  $\gamma$ -secretase. This is not only important for understanding intramembrane proteolysis as a fundamental mechanism in cell biology and cell homeostasis, but may eventually enable the design of new  $\gamma$ -secretase-targeted drugs that act in a substrate-selective or substrate-preferring manner and avoid side effects of the currently used  $\gamma$ -secretase inhibitors in clinical trials for leukemia and AD.

## AUTHOR CONTRIBUTIONS

Marlene Aßfalg, Gökhan Güner, and Stefan F. Lichtenthaler conceived the study. Marlene Aßfalg, Gökhan Güner, and Stefan F. Lichtenthaler with help from Dieter Langosch, Claudia Muhle-Goll, Dmitrij Frishman, Stephan Breimann, and Harald Steiner designed the experiments and analyzed the data, Marlene Aßfalg and Gökhan Güner performed most of the experiments, Gökhan Güner and Stephan A. Müller performed the mass spectrometry analyses, Marlene Aßfalg, Gökhan Güner, and Stefan F. Lichtenthaler wrote the manuscript; all authors contributed to editing and manuscript revisions.

## ACKNOWLEDGMENTS

We thank Katrin Moschke for excellent technical help. This work was funded by the Deutsche Forschungsgemeinschaft (DFG, German Research Foundation) through projects within 263531414/FOR2290 (SFL, HS, DL, CMG, DF), and under Germany's Excellence Strategy within the framework of the Munich Cluster for Systems Neurology (EXC

2145 SyNergy – ID 390857198). CMG thanks the HGF program Information (43.35.02) for financial support. Open Access funding enabled and organized by Projekt DEAL.


## DISCLOSURES

The authors declare to have no conflict of interest.

## DATA AVAILABILITY STATEMENT

The mass spectrometry proteomics data have been deposited to the ProteomeXchange Consortium via the PRIDE<sup>63</sup> partner repository with the dataset identifier PXD045701. Username: [reviewer\\_pxd045701@ebi.ac.uk](mailto:reviewer_pxd045701@ebi.ac.uk). Password: y05rxvznz.

## ORCID

Stefan F. Lichtenthaler  <https://orcid.org/0000-0003-2211-2575>

## REFERENCES

- Brown MS, Ye J, Rawson RB, Goldstein JL. Regulated intramembrane proteolysis. *Cell*. 2000;100:391-398.
- Kühnle N, Dederer V, Lemberg MK. Intramembrane proteolysis at a glance: from signalling to protein degradation. *J Cell Sci*. 2019;132:jcs217745.
- Lichtenthaler SF, Lemberg MK, Fluhrer R. Proteolytic ectodomain shedding of membrane proteins in mammals—hardware, concepts, and recent developments. *EMBO J*. 2018;37:e99456.
- Escamilla-Ayala A, Wouters R, Sannerud R, Annaert W. Contribution of the presenilins in the cell biology, structure and function of  $\gamma$ -secretase. *Semin Cell Dev Biol*. 2020;105:12-26.
- Medoro A, Bartollino S, Mignogna D, et al. Complexity and selectivity of gamma-secretase cleavage on multiple substrates: consequences in Alzheimer's disease and cancer. *J Alzheimers Dis*. 2018;61:1-15.
- Edbauer D, Winkler E, Regula JT, Pesold B, Steiner H, Haass C. Reconstitution of gamma-secretase activity. *Nat Cell Biol*. 2003;5:486-488.
- Gounder M, Ratan R, Alcindor T, et al. Nirogacestat, a gamma-secretase inhibitor for desmoid tumors. *N Engl J Med*. 2023;388:898-912.
- Kaushik B, Pal D, Saha S. Gamma secretase inhibitor: therapeutic target via NOTCH signaling in T cell acute lymphoblastic leukemia. *Curr Drug Targets*. 2021;22:1789-1798.
- Voytyuk I, De Strooper B, Chavez-Gutierrez L. Modulation of gamma- and beta-secretases as early prevention against Alzheimer's disease. *Biol Psychiatry*. 2018;83:320-327.
- Wolfe MS. Unraveling the complexity of  $\gamma$ -secretase. *Semin Cell Dev Biol*. 2020;105:3-11.
- Güner G, Lichtenthaler SF. The substrate repertoire of  $\gamma$ -secretase/presenilin. *Semin Cell Dev Biol*. 2020;105:27-42.
- Chavez-Gutierrez L, Szaruga M. Mechanisms of neurodegeneration – insights from familial Alzheimer's disease. *Semin Cell Dev Biol*. 2020;105:75-85.
- Werner NT, Hogel P, Guner G, et al. Cooperation of N- and C-terminal substrate transmembrane domain segments in intramembrane proteolysis by gamma-secretase. *Commun Biol*. 2023;6:177.
- Steiner A, Schlepckow K, Brunner B, Steiner H, Haass C, Hagn F. Gamma-secretase cleavage of the Alzheimer risk factor TREM2 is determined by its intrinsic structural dynamics. *EMBO J*. 2020;39:e104247.
- Petit D, Hitzentberger M, Lismont S, et al. Extracellular interface between APP and Nicastrin regulates Abeta length and response to gamma-secretase modulators. *EMBO J*. 2019;38:e101494.
- Bolduc DM, Montagna DR, Gu Y, Selkoe DJ, Wolfe MS. Nicastrin functions to sterically hinder gamma-secretase-substrate interactions driven by substrate transmembrane domain. *Proc Natl Acad Sci U S A*. 2016;113:E509-E518.
- Struhl G, Adachi A. Requirements for presenilin-dependent cleavage of notch and other transmembrane proteins. *Mol Cell*. 2000;6:625-636.
- Schauenburg L, Liebsch F, Eravci M, Mayer MC, Weise C, Multhaup G. APLP1 is endoproteolytically cleaved by gamma-secretase without previous ectodomain shedding. *Sci Rep*. 2018;8:1916.
- De Strooper B. Nicastrin: gatekeeper of the gamma-secretase complex. *Cell*. 2005;122:318-320.
- Zhou R, Yang G, Guo X, Zhou Q, Lei J, Shi Y. Recognition of the amyloid precursor protein by human gamma-secretase. *Science*. 2019;363:eaaw0930.
- Laurent SA, Hoffmann FS, Kuhn PH, et al.  $\gamma$ -Secretase directly sheds the survival receptor BCMA from plasma cells. *Nat Commun*. 2015;6:7333.
- Vevea JD, Kusick GF, Courtney KC, Chen E, Watanabe S, Chapman ER. Synaptotagmin 7 is targeted to the axonal plasma membrane through gamma-secretase processing to promote synaptic vesicle docking in mouse hippocampal neurons. *eLife*. 2021;10:e67261.
- Guner G, Assfalg M, Zhao K, et al. Proteolytically generated soluble Tweak receptor Fn14 is a blood biomarker for gamma-secretase activity. *EMBO Mol Med*. 2022;14:e16084.
- Hemming ML, Elias JE, Gygi SP, Selkoe DJ. Proteomic profiling of  $\gamma$ -secretase substrates and mapping of substrate requirements. *PLoS Biol*. 2008;6:e257.
- Schagger H. Tricine-SDS-PAGE. *Nat Protoc*. 2006;1:16-22.
- Sastre M, Steiner H, Fuchs K, et al. Presenilin-dependent gamma-secretase processing of beta-amyloid precursor protein at a site corresponding to the S3 cleavage of Notch. *EMBO Rep*. 2001;2:835-841.
- Papadopoulou AA, Muller SA, Mentrup T, et al. Signal peptide peptidase-like 2c impairs vesicular transport and cleaves SNARE proteins. *EMBO Rep*. 2019;20:e46451.
- Wisniewski JR, Zougman A, Nagaraj N, Mann M. Universal sample preparation method for proteome analysis. *Nat Methods*. 2009;6:359-362.
- Cox J, Hein MY, Luber CA, Paron I, Nagaraj N, Mann M. Accurate proteome-wide label-free quantification by delayed normalization and maximal peptide ratio extraction, termed MaxLFQ. *Mol Cell Proteomics*. 2014;13:2513-2526.
- Tyanova S, Cox J. Perseus: a bioinformatics platform for integrative analysis of proteomics data in cancer research. *Methods Mol Biol*. 2018;1711:133-148.
- Tusher VG, Tibshirani R, Chu G. Significance analysis of microarrays applied to the ionizing radiation response. *Proc Natl Acad Sci U S A*. 2001;98:5116-5121.



32. Percher A, Thimon E, Hang H. Mass-tag labeling using acyl-PEG exchange for the determination of endogenous protein S-fatty acylation. *Curr Protoc Protein Sci.* 2017;89:14.17.1-14.17.11.
33. Dovey HF, John V, Anderson JP, et al. Functional gamma-secretase inhibitors reduce beta-amyloid peptide levels in brain. *J Neurochem.* 2001;76:173-181.
34. Kall L, Krogh A, Sonnhammer EL. Advantages of combined transmembrane topology and signal peptide prediction—the Phobius web server. *Nucleic Acids Res.* 2007;35:W429-W432.
35. Meyer DJ, Bijlani S, de Sautu M, et al. FXYP protein isoforms differentially modulate human Na/K pump function. *J Gen Physiol.* 2020;152:e202012660.
36. Geering K. Function of FXYP proteins, regulators of Na, K-ATPase. *J Bioenerg Biomembr.* 2005;37:387-392.
37. Itoh S, Itoh F. TMEPAI family: involvement in regulation of multiple signalling pathways. *J Biochem.* 2018;164:195-204.
38. Chen Y, Huang S, Guo R, Chen D. Metadherin-mediated mechanisms in human malignancies. *Biomark Med.* 2021;15:1769-1783.
39. Smith VE, Franklyn JA, McCabe CJ. Expression and function of the novel proto-oncogene PBF in thyroid cancer: a new target for augmenting radioiodine uptake. *J Endocrinol.* 2011;210:157-163.
40. Rudan Njavro J, Klotz J, Dislich B, et al. Mouse brain proteomics establishes MDGA1 and CACHD1 as in vivo substrates of the Alzheimer protease BACE1. *FASEB J.* 2020;34:2465-2482.
41. Rodenburg RNP, Snijder J, van de Waterbeemd M, et al. Stochastic palmitoylation of accessible cysteines in membrane proteins revealed by native mass spectrometry. *Nat Commun.* 2017;8:1280.
42. Blanc M, David F, Abrami L, et al. SwissPalm: protein palmitoylation database. *FI000Res.* 2015;4:261.
43. Blanc M, David FPA, van der Goot FG. SwissPalm 2: protein S-palmitoylation database. *Methods Mol Biol.* 2019;2009:203-214.
44. Lan T, Delalande C, Dickinson BC. Inhibitors of DHHC family proteins. *Curr Opin Chem Biol.* 2021;65:118-125.
45. Andrew RJ, Fernandez CG, Stanley M, et al. Lack of BACE1 S-palmitoylation reduces amyloid burden and mitigates memory deficits in transgenic mouse models of Alzheimer's disease. *Proc Natl Acad Sci U S A.* 2017;114:E9665-E9674.
46. Jansen M, Beaumelle B. How palmitoylation affects trafficking and signaling of membrane receptors. *Biol Cell.* 2022;114(2):61-72.
47. Yang G, Zhou R, Zhou Q, et al. Structural basis of Notch recognition by human gamma-secretase. *Nature.* 2019;565:192-197.
48. Krogh A, Larsson B, von Heijne G, Sonnhammer EL. Predicting transmembrane protein topology with a hidden Markov model: application to complete genomes. *J Mol Biol.* 2001;305:567-580.
49. Bouza AA, Philippe JM, Edokobi N, et al. Sodium channel  $\beta$ 1 subunits are post-translationally modified by tyrosine phosphorylation, S-palmitoylation, and regulated intramembrane proteolysis. *J Biol Chem.* 2020;295:10380-10393.
50. Stoeck A, Shang L, Dempsey PJ. Sequential and gamma-secretase-dependent processing of the betacellulin precursor generates a palmitoylated intracellular-domain fragment that inhibits cell growth. *J Cell Sci.* 2010;123:2319-2331.
51. Underwood CK, Reid K, May LM, Bartlett PF, Coulson EJ. Palmitoylation of the C-terminal fragment of p75(NTR) regulates death signaling and is required for subsequent cleavage by gamma-secretase. *Mol Cell Neurosci.* 2008;37:346-358.
52. Cheng H, Vetrivel KS, Drisdell RC, et al. S-palmitoylation of gamma-secretase subunits nicastrin and APH-1. *J Biol Chem.* 2009;284:1373-1384.
53. Fukumori A, Steiner H. Substrate recruitment of gamma-secretase and mechanism of clinical presenilin mutations revealed by photoaffinity mapping. *EMBO J.* 2016;35:1628-1643.
54. Murphy MP, Hickman LJ, Eckman CB, Uljon SN, Wang R, Golde TE.  $\gamma$ -Secretase, evidence for multiple proteolytic activities and influence of membrane positioning of substrate on generation of amyloid beta peptides of varying length. *J Biol Chem.* 1999;274:11914-11923.
55. Lichtenthaler SF, Ida N, Multhaup G, Masters CL, Beyreuther K. Mutations in the transmembrane domain of APP altering gamma-secretase specificity. *Biochemistry.* 1997;36:15396-15403.
56. Tischer E, Cordell B. Beta-amyloid precursor protein. Location of transmembrane domain and specificity of gamma-secretase cleavage. *J Biol Chem.* 1996;271:21914-21919.
57. Lichtenthaler SF, Behr D, Grimm HS, et al. The intramembrane cleavage site of the amyloid precursor protein depends on the length of its transmembrane domain. *Proc Natl Acad Sci U S A.* 2002;99:1365-1370.
58. Xu TH, Yan Y, Kang Y, Jiang Y, Melcher K, Xu HE. Alzheimer's disease-associated mutations increase amyloid precursor protein resistance to gamma-secretase cleavage and the A $\beta$ 42/A $\beta$ 40 ratio. *Cell Discov.* 2016;2:16026.
59. Bolduc DM, Montagna DR, Seghers MC, Wolfe MS, Selkoe DJ. The amyloid-beta forming tripeptide cleavage mechanism of gamma-secretase. *eLife.* 2016;5:e17578.
60. Fernandez MA, Biette KM, Dolios G, Seth D, Wang R, Wolfe MS. Transmembrane substrate determinants for gamma-secretase processing of APP CTF $\beta$ . *Biochemistry.* 2016;55:5675-5688.
61. Ortner M, Guschtschin-Schmidt N, Stelzer W, Muhle-Goll C, Langosch D. Permissive conformations of a transmembrane helix allow intramembrane proteolysis by gamma-secretase. *J Mol Biol.* 2023;435:168218.
62. Gotz A, Mylonas N, Hogel P, et al. Modulating hinge flexibility in the APP transmembrane domain alters gamma-secretase cleavage. *Biophys J.* 2019;116:2103-2120.
63. Perez-Riverol Y, Bai J, Bandla C, et al. The PRIDE database resources in 2022: a hub for mass spectrometry-based proteomics evidences. *Nucleic Acids Res.* 2022;50:D543-D552.

## SUPPORTING INFORMATION

Additional supporting information can be found online in the Supporting Information section at the end of this article.

**How to cite this article:** Aßfalg M, Güner G, Müller SA, et al. Cleavage efficiency of the intramembrane protease  $\gamma$ -secretase is reduced by the palmitoylation of a substrate's transmembrane domain. *The FASEB Journal.* 2024;38:e23442. doi:[10.1096/fj.202302152R](https://doi.org/10.1096/fj.202302152R)